UCSF
UC San Francisco Electronic Theses and Dissertations

Title
Detection of white spot lesions around orthodontic brackets using polarization-sensitive optical coherence tomography

Permalink
https://escholarship.org/uc/item/3381r17c

Author
Chong, Sherri Lyn

Publication Date
2006

Peer reviewed|Thesis/dissertation

eScholarship.org Powered by the California Digital Library
University of California

UC Fran RA

Acknowledgements

Thank you to Dr. Daniel Fried for the opportunity to complete this master's project in his laboratory, and for the continued support and guidance along the way. I was able to explore a topic in orthodontics that clinicians face every day in their practices. Early detection of white spot lesions can vastly improve patient esthetics and satisfaction with orthodontic treatment.

Thank you also to Patara Ngaotheppitak for her help on a daily basis with all of the lab procedures, and for her willingness to provide assistance whenever it was needed.

Dr. Arthur Miller was not only our research class instructor, but he also provided much needed encouragement during this adventure. His positive outlook brightened the most difficult day.

I am grateful to my committee members, Dr. Fried, Dr. John Featherstone, and Dr. Miller for taking the time to review and critique my thesis.

Final thanks to Dave Nasharr, former Ormco representative, for providing the Enlight adhesive and brackets.

UCSF LIBRARY

ABSTRACT

The main purpose of this study was to determine whether a light detection system, polarization-sensitive optical coherence tomography (PS-OCT), is able to accurately track the initiation and progression of early demineralized lesions around orthodontic bracket bases. Another goal of the study was to analyze the protective effects of different fluoride modalities in preventing decay around bracket bases. Sixty human molar samples used for this *in vitro* study were divided into four groups of fifteen. The groups consisted of the control (Ormco Enlight® adhesive, no fluoride), fluoride in solution (2ppm fluoride), fluoride sealant (Reliance Proseal®), and glass ionomer adhesive (Fuji Ortho LC®). Each section was mounted in acrylic, then scanned with the PS-OCT system at time 0 (before and after bracket placement), and subsequently at days 3, 6, 9, 12, and 15. Quantitative analysis demonstrated that PS-OCT was effective in showing nondestructively that the various fluoride modalities significantly reduced the lesion severity ($p<0.001$). The fluoride sealant group was significantly more effective than the fluoride in solution group and the glass ionomer group. Digital microradiography (DM) was completed as the gold standard to which the PS-OCT measurements were compared to verify accuracy of detection. Polarized light microscopy (PLM) was used to examine lesion depth. Microradiography and polarized light microscopy verified the presence of the lesion depicted by OCT, and PLM verified the depth of the lesion. This study demonstrates that PS-OCT can potentially be used in the orthodontic clinical setting to monitor the severity of demineralization, and monitor the efficacy of intervention using fluoride-based therapeutic agents.

UCSF LIBRARY

Table of Contents

Title Page i

Acknowledgement ii

Abstract iii

Table of Contents iv

List of Tables vi

List of Figures vii

I. Introduction for Thesis 1

A. Prevalence of dental decay 1

B. Development of demineralization 1

C. Characteristics of decay around orthodontic brackets 1

D. Role of fluoride 2

E. Various modalities of fluoride 2

F. Tooth components 4

G. Conventional diagnostic techniques 5

H. Advanced diagnostic techniques 5

I. Polarization-sensitive optical coherence tomography (PS-OCT) 7

J. Digital microradiography 11

K. Purpose of the study 12

L. Specific aims of the study 12

II. Materials and Methods 13

A. Sample and method of preparation 13

B. PS-OCT system 14

C. Demineralization/remineralization solutions 16

D. PS-OCT scans 17

E. Polarization light microscopy and digital microradiography 17

III. Results 19

A. Descriptive statistics 19

B. Examples from each group 32

UCSF LIBRARY

IV. Discussion **37**

A. Assessment of PS-OCT as imaging method 37

B. Effectiveness of different fluoride modalities 37

C. PS-OCT, PLM, and DM 38

V. Conclusion **42**

VI. References **43**

VII. Appendix **47**

UCSF LIBRARY

List of Tables

Table	Subject	Page
1.	PS-OCT reflectivity data	47
2.	Mean reflectivity and standard deviations for all groups at day 15	20
3.	Difference between mean reflectivity from day 0 to 15 for all groups and standard deviations	22
4.	Average backscattering and standard deviations at days 0, 3, 6, 9, 12, and 15 for the control group	24
5.	Average backscattering and standard deviations at days 0, 3, 6, 9, 12, and 15 for the fluoride in solution group	26
6.	Average backscattering and standard deviations at days 0, 3, 6, 9, 12, and 15 for the fluoride sealant group	27
7.	Average backscattering and standard deviations at days 0, 3, 6, 9, 12, and 15 for the glass ionomer group	29
8.	Microradiography data	49
9.	Polarized light microscopy data (mean depths and standard deviations)	32
10.	Polarized light microscopy data	50

UCSF LIBRARY

List of Figures

Figure	Subject	Page
1.	Diagram of the PS-OCT system	9
2.	Isomet 2000 precision saw	13
3.	Tooth mounted in acrylic block	13
4.	Acrylic block in holder, light beam aimed at tooth sample	14
5.	B-scan from control group with line profiles	15
6.	Bonded brackets with painted varnish	16
7.	Mean reflectivity for all groups at day 15	21
8.	Difference between mean reflectivity from day 0 to 15 for all groups	22
9.	Mean reflectivity at all days for control group (adjacent to bracket base)	24
10.	Mean reflectivity at all days for control group (halfway between side of bracket base and edge of tooth)	25
11.	Mean reflectivity at all days for fluoride in solution group	26
12.	Mean reflectivity at all days for fluoride sealant group	28
13.	Mean reflectivity at all days for glass ionomer group	29
14.	Integrated reflectivity plotted vs. square root of time	30

UCSF LIBRARY

15. PS-OCT, PLM, DM images from control sample 33
16. PS-OCT, PLM, DM images from fluoride in solution sample 34
17. PS-OCT, PLM, DM images from fluoride sealant sample 35
18. PS-OCT, PLM, DM images from glass ionomer sample 36

UCSF LIBRARY

INTRODUCTION

Dental decay was prevalent prior to the addition of fluoride to drinking water in the 1960's and the universal use of fluoridated toothpastes, mouthrinses, and fluoride application in the dental office. Even through the mass introduction of fluoride and emphasis on oral hygiene, dental decay still continues to be a problem, and remains the leading cause of tooth loss in the United States (Chauncey *et al.*, 1989; Kaste *et al.*, 1996; Winn *et al.*, 1996). Smooth surfaces have seen the greatest decline in caries incidence with most of the carious lesions occurring in pits and fissures (White *et al.*, 2000). With orthodontic appliances, the smooth surfaces can become "plaque traps" and the risk of decalcification increases. Maintaining oral hygiene and following the diet regimen are challenging during orthodontic treatment. Noncompliance can lead to a higher prevalence of demineralization seen when removing orthodontic braces.

The development of caries during orthodontic fixed appliance therapy is a significant concern. Demineralization occurs following plaque accumulation around appliances, subsequent acid production (lowers the pH) by bacteria, and acid attack on tooth structure, leading to diffusion of calcium and phosphate ions from enamel (Millett *et al.*, 1999). Early decalcification, demineralization, or "white spot lesions" as they are often referred to, may develop and progress very rapidly around brackets and bands. White spot lesions have been shown to develop within one month around brackets and bands (Ogaard *et al.*, 1992). Such areas of decalcification are called white spot lesions due to the loss of

UCSF LIBRARY

translucency of the enamel in that area. There is no cavitation but it may present as a rough surface (Featherstone *et al.*, 1985). The non-cavitated surface layer is about 40-50μm thick, exhibits less than 20% demineralization, and subsurface layers can be up to 70% demineralized (Featherstone, 1980). The initial appearance is chalky white, but if mineral loss continues, subsurface lesions will result. The white spot may discolor over time due to stains seeping into the large pores (Featherstone *et al.*, 1985; Thylstrup *et al.*, 1994). There is a possibility that white spot lesions may regress or disappear due to surface abrasion, but may still pose an esthetic problem even five years post-treatment (Millett *et al.*, 1999). The incidence of this demineralization after full fixed appliance treatment can be as high as 50% (Pascotto *et al.*, 2004), or as noted elsewhere between 2%-96% of patients (Millett *et al.*, 1999). If these initial lesions are detected early, they can be arrested, or even reversed, by a variety of non-invasive methods including fluoride administration, anti-bacterial rinses, dietary changes, or low-intensity laser irradiation (Featherstone *et al.*, 1985; Featherstone, 1999).

The role of fluoride in preventing or arresting dental decay has been thoroughly studied. There are many possible delivery systems for fluoride including drinking water, toothpastes, rinses, foods and beverages, and application in the dental office. Three mechanisms of fluoride are the antibacterial action of fluoride, inhibition of mineral dissolution, and enhancement of remineralization (Featherstone, 2000). The antibacterial action is expressed when fluoride enters the bacterial cell, interferes with enzymatic activity, thereby slowing down or inhibiting acid production. Fluoride also inhibits dissolution of

UCSF LIBRARY

UC Fran RA

calcium and phosphate in enamel, by dissolving during an acid challenge, preventing the tooth structure from being dissolved (Featherstone, 1990). Another role of fluoride is to bring calcium and phosphate ions together forming a more acid-resistant surface that makes decay less likely to progress (Featherstone, 1990). Daily fluoride should be applied to the surface of the tooth to have the most effect (Featherstone, 1990). Oral hygiene maintenance and a fluoride rinse are usually recommended to orthodontic patients to prevent decalcifications from developing. It has been shown that regular fluoride toothpaste use alone is unable to inhibit the development of lesions around brackets (Ogaard et al., 1992). The use of a neutral 0.05% sodium fluoride rinse along with a fluoride toothpaste can significantly reduce the appearance of white spot lesions, depending on patient compliance (Geiger et al., 1992). The use of a fluoride-releasing adhesive for bonding reduced lesion development around brackets compared to the use of a non fluoride-releasing adhesive (Gorton et al., 2003, Ogaard et al., 1992, Pascotto et al., 2004, Marcusson et al, 1997). Resin-modified glass ionomer cement releases fluoride but also has greater adhesive strength than conventional glass ionomer (Pascotto et al., 2004). Most of the fluoride is released during the first day after bonding, but there is continued release over a few months (Millett et al., 1999). The fluoride from the adhesive acts locally, so the caries-inhibiting effect is not due to an increase in the fluoride level in saliva (Ogaard et al., 1997). In a high concentration fluoride solution, glass ionomer cements can actually absorb the fluoride from solution and be a continuous source of fluoride over time (Millett et al., 1999). The amount of

UCSF LIBRARY

UC Fran RA

fluoride release increases as the sodium fluoride content in the adhesive increases (Donly et al., 2002). Topical fluoride application following initial acid etching of the tooth has been shown to be an additional source of fluoride without altering the bond strength of the adhesive (Hirce et al., 1980).

The four primary components of the human tooth are enamel, dentin, cementum and pulp. Enamel is a porous material and consists of mainly calcium salts forming hydroxyapatite crystals arranged perpendicular to the tooth surface (Featherstone, 1980). Some of these crystals form enamel rods or prisms, which are the structural units of enamel. The rods are orderly-arranged parallel and perpendicular to the tooth surface (Wang *et al.*, 1999). The structural arrangement accounts for the negative intrinsic birefringence of enamel (Featherstone *et al.*, 1985). Intrinsic birefringence is due to the mineral composition of the tissue. When caries is present, the pores in enamel enlarge and when filled with a mineral that has a different refractive index from enamel, positive form birefringence is produced (Featherstone *et al.*, 1985). The total birefringence is a combination of these two types (Featherstone *et al.*, 1985). Protein is interspersed between the rods and composes about 2% of enamel.

Dentin is composed of 30% organic material (collagen fibrils), 50% inorganic material (carbonated hydroxyapatite crystals), and 20% water. Dentin is composed of units called dentinal tubules. The tubules radiate from the pulp to the dentinoenamel junction (DEJ) in an S-shaped fashion, and narrow as they approach the DEJ. The collagen fibrils surrounding the tubules are perpendicular to the tubules and roughly parallel to the tooth surface. In dentin it is the tubules

UCSF LIBRARY

UC Fran RA

that are the principle scatterer of the light, not the mineral crystals (ten Bosch *et al.*, 1991). The greater light scattering and absorption in dentin compared to enamel is responsible for dentin's yellow appearance, compared to the translucent color of enamel (Feldchtein *et al.*, 1998). At the DEJ, the tubules are oriented almost perpendicular to the propagation direction, and the backscattering signal is strong with increasing depth (Wang *et al.*, 1999).

Initially, light was utilized for imaging caries. Conventional diagnostic radiographic techniques then became the imaging method of choice. Radiographs can adequately diagnose large carious lesions, but do not work as well for noncavitated, root, or secondary caries. Moreover, lesion depth cannot be accurately quantified. Dental x-rays also release ionizing radiation so can rarely be justified for frequent monitoring. Early detection and determining the extent of decay are extremely important. Being able to monitor the progression of lesions is essential during treatment extended over a long time period such as in orthodontics. With the dental explorer and radiographs, up to 60% of lesions can be missed (Rousseau *et al.*, 2002). The sensitivity of the explorer is only about 50-60% (Eakle *et al.*, 2003). Due to these limitations with conventional methods of diagnosis, there has been a return to utilization of light for detection. Exploring optical imaging is of ever increasing importance. Advanced methods such as FOTI (fiber-optic transillumination), DIFOTI (digital imaging fiber-optic transillumination), Diagnodent, and QLF (quantitative laser fluorescence) all have been used *in vivo*. FOTI and DIFOTI both utilize light in the visible range for illumination, which is limited by increased scattering and decreased resolution

UCSF LIBRARY

and penetration depth. One of the advantages of DIFOTI is the standardization of the incident light, which allows for more accurate reproducibility of the images at different time points and with different operators (Zero *et al.*, 1992). DIFOTI is suggested to be able to detect inter-proximal lesions but is not as effective at detecting occlusal lesions (Fried *et al.*, 2002). Diagnodent uses near infrared light (655nm) to detect fluorescence from porphyrins produced by bacteria (Fried *et al.*, 2002; Eakle *et al.*, 2003). Diagnodent detects caries after it has accumulated a significant amount of bacteria and has involved dentin (Fried *et al.*, 2002). Diagnodent is not accurate in detecting enamel lesions and in determining lesion severity and depth (Fried *et al.*, 2002; Eakle *et al.*, 2003), but has been found to be useful if combined with visual examination (Anttonen et al., 2003). QLF involves a blue-green light (488nm) emitted from an argon-ion laser (Hafstroem-Bjoerkman *et al.*, 1992). Currently, QLF uses filtered light, not the argon-ion laser. QLF involves a relationship between the extent of enamel demineralization and loss of fluorescence intensity from the underlying dentin (Hafstroem-Bjoerkman *et al.*, 1992). A high fluorescence intensity signifies sound enamel, whereas a low fluorescence intensity is representative of carious enamel (Hafstroem-Bjoerkman *et al.*, 1992). When this QLF method was compared to microradiography, the demineralization measurements were strongly correlated (Hafstroem-Bjoerkman *et al.*, 1992). QLF can detect minute changes in decalcification when compared to diagnostic ultrasound (Fontana *et al.*, 1996). Ultrasound uses pulse-echo techniques to detect decay (Fontana *et al.*, 1996). QLF has been shown to be suitable for monitoring early enamel

UCSF LIBRARY

demineralization in orthodontic patients (Angmar-Manssona et al., 99). QLF can only image smooth surfaces, not interproximal or occlusal, and cannot detect subsurface lesions (Fried *et al.*, 2002). All of these optical methods have limitations regarding the area of the tooth that can be imaged and ability to detect subsurface lesions. An ideal optical method is needed that can detect subsurface lesions, can image all surfaces, and can be used frequently to monitor lesion progression.

Conventional optical coherence tomography does not account for different polarization states, so resolution of the images is decreased (Wang *et al.*, 1999). The significant surface reflection is incorporated into the one polarization state image and detection of caries vs. surface reflection is blurred. Birefringence is also a problem due to artifacts such as banding obscuring the detection of early caries (Jones *et al.*, 2004).

The optical coherence tomography (OCT) system was first introduced as a biological imaging system by Huang in 1991 (Huang *et al.*, 1991). Optical coherence tomography is a non-invasive, high resolution imaging system that measures backscattered light to create cross-sectional images of biological structures. OCT is similar to ultrasound, providing real-time structural imaging, but ultrasound involves sound waves, whereas OCT involves light waves. PS-OCT is a version of OCT in which the polarized reference state of the backscattered light is incorporated. PS-OCT has been used to image the eye, skin, digestive tract, dysplasias, and carcinoma in situ (de Boer et al., 1999). PS-OCT can also provide information regarding dental structures and more

UCSF LIBRARY

specifically, caries presence and progression. Colston (Colston et al., 1997, 1998a, 1998b) was the first to image oral soft and hard tissues with conventional OCT. Baumgartner (Baumgartner *et al.*, 1998; Baumgartner *et al.*, 1999; Baumgartner *et al.*, 2000) was the first to present a polarized image of caries, but the penetration depth was low. Tooth substance is not altered when scanned, so more than single measurements are possible. PS-OCT can image subsurface caries by detecting an increase in depolarization and reflectivity (backscattering). Within a certain wavelength range, as the backscattering decreases, the penetration increases. PS-OCT utilizes near-infrared light (830-1550nm, functioning best near 1310nm), increasing the penetration depth over the visible range. Multiple studies have been done to determine the ideal wavelength. Fried (Fried *et al.*, 1995) demonstrated that in the visible and near infrared zones, dentin strongly scatters light. The scattering in enamel decreases with increasing wavelengths. It has been shown that the magnitude of scattering at 1310nm and 1550nm is more than 30 times lower than at visible light wavelengths (Jones *et al.*, 2002). Beyond 1550nm, scattering does not decrease any further and penetration does not increase any further because of the increasing absorption by water in the enamel (Fried *et al.*, 2002; Hale *et al.*, 1973). Enamel is nearly transparent in the IR range, and can be imaged to a depth of 2-3mm with 10-30μm resolution. The imaging depth is determined by the amount of light that penetrates the tissue and the image acquisition time (Otis *et al.*, 2000). Feldchtein ((Feldchtein *et al.*, 1998) imaged enamel, dentin, caries in both enamel and dentin, and restorations with high resolution at 830nm and 1280nm.

UCSF LIBRARY

Everett (Everett *et al.*, 1999) used a high power 1310nm broadband source and PS-OCT to display polarized images. Otis (Otis *et al.*, 2000) also showed that a 1310nm imaging system is superior to one that operates at 850nm. The optical properties of enamel and dentin change with demineralization and remineralization, the extent of which can be detected by the PS-OCT system. The scattering coefficient of dentin is higher than enamel, so the penetration depth is less than enamel (Fried *et al.*, 2002). The penetration depth can vary within the same tooth depending on the topographical differences (Jones *et al.*, 2004). Scattering signals generated are higher at tissue interfaces, such as the DEJ (Otis et al., 00).

The PS-OCT system is illustrated in Fig. 1 (Jones *et al.*, 2004). Light is emitted from the low coherence, superluminescent diode source (SLED), travels through the polarizer (P), and is divided by a beam splitter (50/50) into sample and reference arms. The piezoelectric fiber stretchers (pzm) vary the path length differences between the sample and reference arms so the signal will coincide at the detector. Backscattered light from the sample tissue and reflections from the reference mirror merge at the splitter and are interpreted by the photodetector. The polarizing beamsplitter (PBS) splits the light into two axes, fast (perpendicular) and slow (parallel).

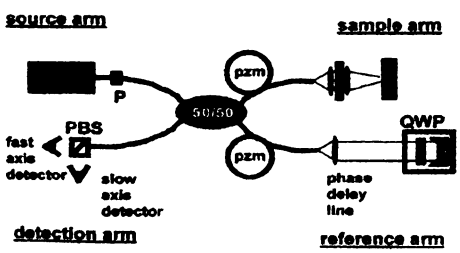

Figure 1. Diagram of the PS-OCT system. Light is emitted by SLED, and is divided by a beam splitter (50/50) into the sample and reference arms. Backscattered light from the tissue and mirror merge at the splitter and are interpreted by the photodetector. The polarizing beamsplitter (PBS) splits the light into the fast and slow axes.

UCSF LIBRARY

Backscattering, or reflectivity, is measured in units of decibels (dB). Axial interferometric signals are generated from points on the tissue, expressed as a-scans, and these signals are combined to form a two-dimensional OCT image, or b-scan, by the detector. The coordinates of the a-scan are decibels on the y-axis and pixels on the x-axis. Decibels (dB) are expressed as a logarithmic scale and the maximum pixel amount is 1000 which is equal to a depth of 5.74mm through the tooth. Signal is detected only when reflections from the sample and reference arms nearly coincide at the detector (Huang *et al.*, 1991). The detector consists of two parts, the slow/parallel/p-axis and the fast/perpendicular/s-axis. The PS-OCT system images in the parallel and perpendicular axes, enhancing the image contrast and reducing the interference of reflections at surface interfaces and native birefringence of enamel rods (Fried *et al.*, 2002; Jones *et al.*, 2004). The slow axis image includes all of the backscattered light from the tooth, including surface reflections, created by the air-enamel interface (Fried *et al.*, 2002). This can mask surface or subsurface scattering and create artifacts (spikes) in the image (Fried *et al.*, 2002). The fast axis image measures depolarized light in the perpendicular polarization state, and does not detect the strong surface reflections, giving a much clearer image of the scattering of enamel and dentin.

It has been shown that PS-OCT can successfully detect artificial lesion progression on occlusal surfaces and under sealants and composite restorations (Jones *et al.*, 2004). Defects between the sealant/composite and the tooth surface can create strong reflections (Jones *et al.*, 2004). Due to the polarization

UCSF LIBRARY

UC Fran RA

component of PS-OCT, strong surface reflection is not confused with actual demineralization occurring (Jones *et al.*, 2004). Surface reflection is not detected in the perpendicular or S-axis because the light is not depolarized with reflection at zero degree incidence. For sound enamel, the parallel axis signal is high due to surface reflection and the perpendicular axis signal is low because it only consists of the polarization rotation due to enamel birefringence. With caries, the perpendicular axis signal is high, similar to the parallel axis, due to the intense depolarization. This occurs with the increase in light scattering of 2-3 orders of magnitude. The polarization rotation with sound enamel is so low in the perpendicular axis that when quantifying the signal from a carious lesion, only the reflectivity or backscattering from the carious lesion at that stage needs to be accounted for. The subtraction-based technique where day 0 reflectivity needs to be subtracted from the current caries reflectivity does not need to be done. This becomes important in the clinical setting where the sound day-0 signal is unknown. The perpendicular-axis image is insensitive to the different topographies of the tooth (more significant for occlusal surfaces than smooth surfaces). The subtraction method does need to be performed for the parallel axis, to eliminate surface reflection.

High resolution digital microradiography is an invasive procedure used as the gold standard to quantify demineralization for comparison with OCT. Microradiography measures mineral loss or gain in the enamel and dentin of the sample teeth due to a change in x-ray attenuation. Transverse thin sections are cut (200μm), which can be examined with a polarized light microscope to

UCSF LIBRARY

UC Fran RA

reference the lesion depth. The microscope is connected to a high resolution digital camera to compare the actual depth of the lesion to the PS-OCT images. There is a high success rate of sectioning 200μm-thick samples, but it is more difficult to properly assess lesion depth (Jones *et al.*, 2004). The relative mineral loss (vol% x μm), ΔZ, is calculated by comparing the difference between sound and carious tooth structure (Jones *et al.*, 2004). The direct comparison of 200 μm microradiography sections to 20 μm PS-OCT sections poses challenges, but thicker microradiography sections are necessary to prevent destruction of the sections.

Objectives and Hypothesis

The purpose of the current study was to track carious lesion progression, reversal, and arrestment with the PS-OCT system over a 15-day demineralization-remineralization cycle. The hypothesis to be tested was that PS-OCT can nondestructively measure and quantify the efficacy of fluoride, in the form of glass ionomer adhesive, fluoride sealant, and fluoride in solution, in inhibiting the development of white spot lesions around orthodontic bracket bases. The specific aims of the study were two-fold: develop an imaging method to track the development of white spot lesions around orthodontic brackets, and to test the efficacy of a fluoride-releasing adhesive (glass ionomer), fluoride sealant, and fluoride in solution in preventing simulated decay around orthodontic brackets.

UCSF LIBRARY

UC Fran RA

MATERIALS AND METHODS

Following root resection, 30 human molars were sectioned into buccal and lingual halves with the Isomet 2000 precision saw and copious irrigation (Fig. 2). The halved molars were mounted flat on acrylic blocks of similar dimension, with the buccal (or lingual) side away from the acrylic and the halved tooth centered (Fig. 3). Each exposed surface was cleaned with an aluminum oxide slurry to ensure a clean surface for imaging and bonding. Teeth were stored in a moist environment to maintain tissue hydration, and 0.1% thymol was added to prevent bacterial growth.

Figure 2. Isomet 2000 precision saw used to section molars into buccal and lingual halves.

Figure 3. An example of a halved molar mounted in an acrylic block. Each half was polished with a slurry of 1μm aluminum oxide size particles to ensure a clean surface for imaging and bonding.

UCSF LIBRARY

UNIVERSITY OF CALIFORNIA

The PS-OCT system that was used has been thoroughly described by Fried (Fried *et al.*, 2002). An all fiber-based optical coherence domain reflectometer with polarization maintaining optical fiber, piezoelectric fiber stretchers, and two InGaAs detectors was coupled with a 20 MW, 25nm bandwidth superluminescent diode source, emitting light at 1310nm. The tooth sample blocks were scanned individually, first placing the block in a standardized holder, then orienting the light beam so it approximates the center of the tooth (Fig 4a, 4b). The x- and y-coordinates were altered until the beam is aimed at the far left of the tooth and approximately centered vertically. That designated the scan start stage. Six hundred 20μm sections were taken in the x-direction at three 100μm intervals in the y-direction. This cycle was completed three times for each sample to generate the b-scans (Fig. 5). Initial PS-OCT scans were completed to eliminate the possibility of existing caries on the bonding tooth surface, and to serve as control scans. Only weak scattering should result from sound enamel.

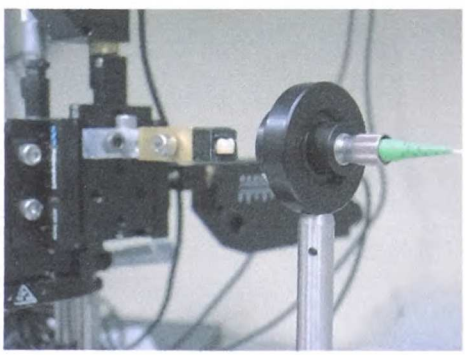

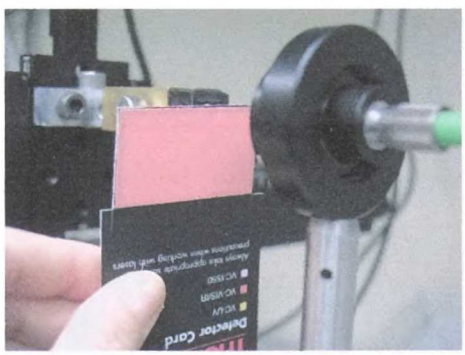

Figures 4a and 4b. Acrylic block is in a standardized holder, and the light beam is oriented to approximate the center of the tooth.

UCSF LIBRARY

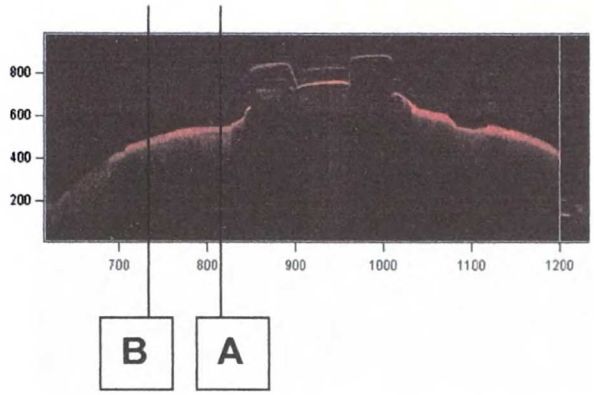

Figure 5. Example of a b-scan from a control group sample with line profiles. (A). line profile taken adjacent to the bracket base.
(B). line profile taken halfway between the side of the bracket base and the edge of the tooth. The left side of the tooth was chosen arbitrarily.

The samples were randomly assigned to one of four groups, each containing 15 human molar halves (n = 60) bonded with metal orthodontic brackets (Ormco) (Fig. 6). The four groups were:

1) *control*: non-fluoride-containing adhesive-bonded brackets (Enlight® adhesive, Ormco)
2) *experimental*: fluoride in solution (2ppm F in solution) with non-fluoride-containing adhesive-bonded brackets (Enlight® adhesive, Ormco)
3) *experimental*: fluoride sealant (Proseal®, Reliance Orthodontic Products) with non-fluoride-containing adhesive-bonded brackets (Enlight® adhesive, Ormco)
4) *experimental*: glass ionomer adhesive-bonded brackets (Fuji Ortho LC® 2-part adhesive, GC America)

UCSF LIBRARY

MAP LIBRARY

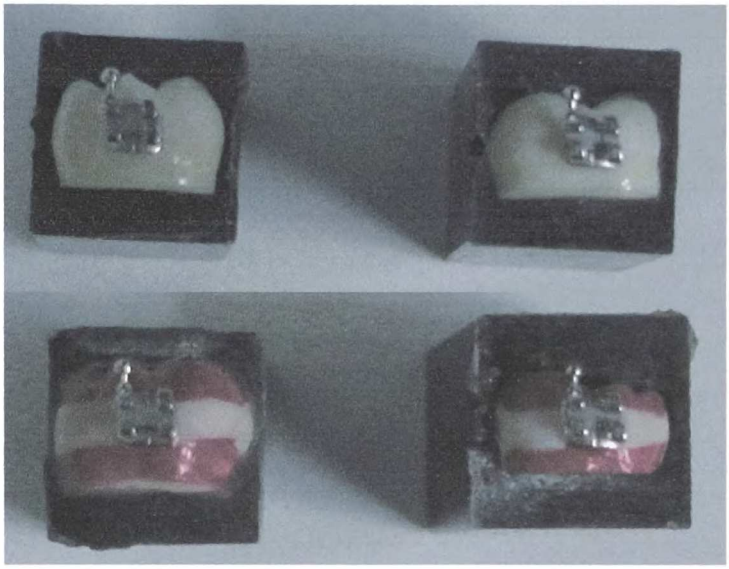

Figure 6. Bonded metal orthodontic brackets (Ormco) with varnish painted over the areas that were not scanned.

Prior to treatment, the exposed surface of each sample was etched with 37% phosphoric acid for 30 seconds, then rinsed with deionized water and air dried with the air syringe. Fluoride was only applied to the samples once at day 0, except for the fluoride in solution group. 2ppm neutral fluoride was added to the remineralization solution for the fluoride in solution group initially and prior to day 9 when the solutions were changed. The fluoride sealant was applied to the tooth surface prior to bonding the bracket. The glass ionomer cement was used instead of the non-fluoride-containing adhesive for the glass ionomer group. The brackets were adapted as close to the tooth surface as possible. The excess cement around the brackets was removed prior to curing with a halogen light for 30 seconds. A second series of scans were taken with the bonded brackets, also to serve as control scans. All groups were subjected to cycles of demineralization and remineralization (pH changes similar to *in vivo*) for a total of

UCSF LIBRARY

BAAP LIBRARY

15 days. The demineralization-remineralization cycling was explained in detail by Featherstone (Featherstone, 90). The samples were exposed to 6 hours of demineralization and 17 hours of remineralization every day for 3 days then b-scans were taken of all samples. This was repeated for 15 days. The demineralization solution consisted of 40 ml aliquots containing 2.0mmol/L calcium, 2.0mmol/L phosphate, and 0.075mol/L acetate at a pH of 4.5 and a temperature of 37°C. The remineralization solution consisted of 20 ml aliquots containing 1.5mmol/L calcium, 0.9mmol/L phosphate, 150mmol/L KCl, and 20mmol/L cacodylate buffer at a pH of 7.0 and a temperature of 37°C. Progressive scans at 3, 6, 9, and 12 days of the cycle were taken to determine the timing of appearance of any white spot lesions. Final scans were taken at 15 days after the demineralization cycles were completed. The solutions were changed prior to the start of day 9 for all groups for relative constancy of the pH levels. A line profile (one point on the b-scan where the backscattering reading will be taken) was subsequently taken on one side adjacent to the bracket base (Fig. 5). The side of the bracket analyzed was determined arbitrarily. Comparison of all the line profiles was used to determine the effectiveness of the PS-OCT system in detecting white spot lesions, and the efficacy of each mechanism of fluoride delivery.

After the PS-OCT scanning, the tooth hemi-sections were serially cut into sections of ~200 μm thickness for polarized light examination and digital quantitative microradiography. The thickness of each section was measured with a digital micrometer with 1 μm resolution. Ideally, thin sections of 80-100 μm

UCSF LIBRARY

UNIV. OF CALIFORNIA LIBRARY

thickness should be used for both PLM and DM, and thinner sections are more desirable for comparison with the 20 μm thick PS-OCT scans. However, enamel is very brittle and difficult to cut into thin sections without fracture, more so for carious sections, and attempts to produce such thin sections would result in an unacceptable high loss rate of samples/sections, therefore we chose a more reliable section thickness of 200 μm. Thin sections were imbibed in water and examined at up to 500x with a polarizing microscope interfaced to a high-resolution digital camera. Thin sections were examined visually using a Westover Scientific Series 7 optical microscope (Westover Scientific, Mill Creek, WA) with an integrated digital camera, Canon EOS Digital Rebel XT (Canon Inc., Tokyo, Japan) and Image Pro Plus® software (Media Cybernetics, Silver Spring, MD). A Moire Ruling with 100 lines per mm was used to calibrate the length measurements on the images. Samples were examined in the brightfield mode with crossed polarizers and a red I plate with 500-nm retardation. Demineralization due to strong scattering caused loss of birefringence in the lesion and it appeared dark. Measurements of lesion depth were made with calibrated image analysis software that is capable of direct length and area measurements.

UCSF LIBRARY

UC Fran
RA
UC Fran
RA
UC Fran
RA

RESULTS

PS-OCT is an effective method for detection of white spot lesions, as verified by digital microradiography and polarized light microscopy. Samples treated by the three fluoride modalities included in this study (fluoride in solution, fluoride sealant, and glass ionomer cement) showed significantly less demineralization when compared to control samples. Over time, there was a large initial increase in demineralization for the control group, which continued to increase then plateaued. For the fluoride in solution group, there was also a large initial increase in demineralization but less than for the control group. After this initial increase, there was a decrease in demineralization over time. The fluoride sealant group showed the least demineralization overall, and did not show the initial increase in demineralization as for the control and fluoride in solution groups. The glass ionomer group did show the initial increase in demineralization, although it was less than the control and fluoride in solution groups. The demineralization then plateaued over time. The results of the PS-OCT measurements, the polarized light microscopic analysis, and digital microradiography are reported in Tables 1-10 and Figures 7-18.

Table 1 (appendix) displays the raw data for the PS-OCT mean reflectivity readings. Multiple analyses were completed to compare the groups and examine the results over time. The mean integrated reflectivity (ΔR [dBxμm]) measured with PS-OCT between the control group and the three groups treated with fluoride was significantly different ($p<0.001$).

UCSF LIBRARY

UC
Fran
RA
UNIV
UNI
UC
Fran
RAF
ORNIA
BRA

Table 2 and Figure 7 show the difference between the average backscattering for each of the four groups at day 15. The mean and standard deviations for each group are as follows: control (350±65), fluoride in solution (194±66), fluoride sealant (110±33), and glass ionomer (170±63). The one-way analysis of variance (ANOVA) followed by the Tukey-Kramer post-hoc multiple comparisons test was used. The control group had a significantly greater integrated reflectivity than the other three groups ($p<0.001$). The fluoride sealant group showed significantly less reflectivity than the other two fluoride groups, but there was no significant difference between the fluoride in solution and glass ionomer groups.

Table 2. Average backscattering and standard deviations for each of the four groups at day 15. All comparisons are statistically significant except for the fluoride in solution and glass ionomer.

Group	Number of Points	Mean	SD	Comparison	p-value
Control	15	350	65	Control vs. F in Solution	p<0.001
F in Solution	15	194	66	Control vs. F Sealant	p<0.001
F Sealant	15	110	33	Control vs. Glass Ionomer	p<0.001
Glass Ionomer	15	169	63	F in Solution vs. F Sealant	p<0.01
				F in Solution vs. Glass Ionomer	p>0.05 ns
				F Sealant vs. Glass Ionomer	p<0.05

UNIVERSITY OF CALIFORNIA

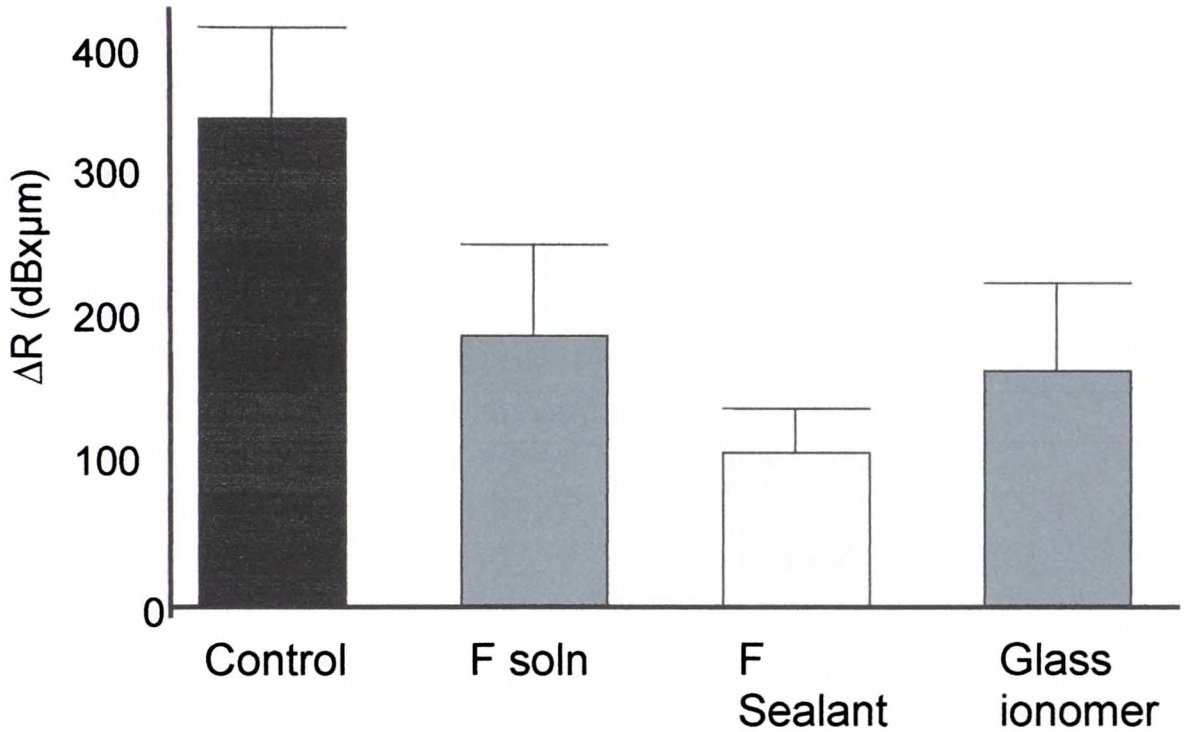

Figure 7. Mean reflectivity (ΔR) for the control, fluoride in solution, fluoride sealant, and glass ionomer groups at day 15. The error bars represent standard deviations. The darkly-shaded control group is significantly different from the three fluoride groups ($p<0.001$), and the non-shaded fluoride sealant group is significantly different from the other three groups.

Table 3 and Figure 8 display the difference between the mean reflectivity for each of the four groups at day 15 and day 0. The mean and standard deviations for each group are as follows: control (292±68), fluoride in solution (106±76), fluoride sealant (58±62), and glass ionomer (114±52). The one-way analysis of variance (ANOVA) followed by the Tukey-Kramer post-hoc multiple comparisons test was used. The mineral loss was greatest for the control group, and significantly less for the fluoride groups. There was no significant difference among the fluoride groups.

UCSF LIBRARY

Table 3. The difference between the average backscattering and standard deviations for each of the four groups at day 0 and day 15. The difference was statistically significant between the control group and the three fluoride groups, and not significant among the fluoride groups.

Group	# of Points	Mean	SD	Comparison	p-value
Control	15	292	68	Control vs. F in Solution	p<0.001
F in Solution	15	106	76	Control vs. F Sealant	p<0.001
F Sealant	15	58	62	Control vs. Glass Ionomer	p<0.001
Glass Ionomer	15	114	52	F in Solution vs. F Sealant	p>0.05 ns
				F in Solution vs. Glass Ionomer	p>0.05 ns
				F Sealant vs. Glass Ionomer	p>0.05 ns

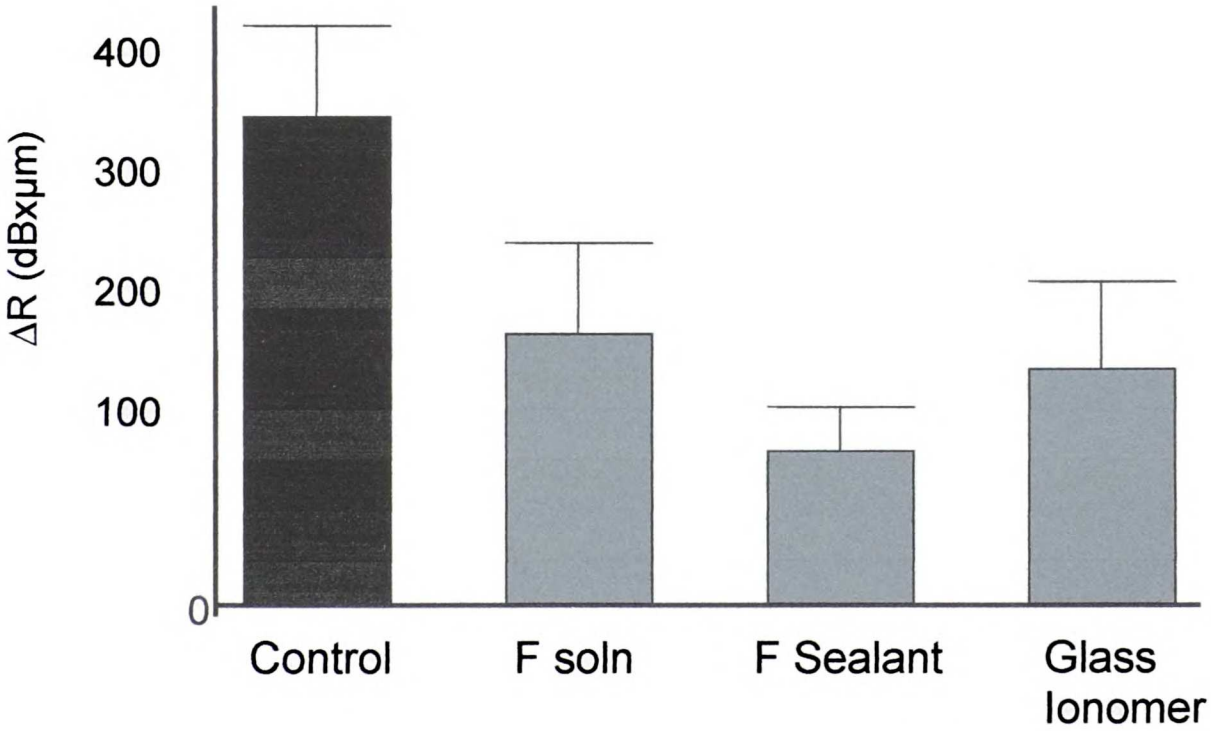

Figure 8. Mean reflectivity (ΔR) for the control, fluoride in solution, fluoride sealant, and glass ionomer groups between days 0 and 15. The error bars represent standard deviations. The darkly-shaded control group was significantly different from the three fluoride groups (p<0.001). There was no significant difference among the fluoride groups.

UNIVERSITY OF CALIFORNIA LIBRARY

Each group was analyzed at the six time points. Repeated-measures analysis of variance (ANOVA) followed by the Tukey-Kramer post-hoc multiple comparisons test was used. Figure 9 shows the average backscattering at days 0, 3, 6, 9, 12, and 15 for the control group when the scans were taken adjacent to the bracket base. There was no significant difference in reflectivity over time. Table 4 and Figure 10 display the average backscattering at days 0, 3, 6, 9, 12, and 15 for the control group when the scans were taken halfway between the side of the bracket base and the edge of the tooth. In Figure 10, the greatest increase in demineralization was seen very early on from day 0 to day 3. The demineralization plateaus with a slight decrease at day 12 and a slight increase at day 15. The means and standard deviations for each time point are as follows: day 0 (58 ±35), day 3 (247±66), day 6 (306±57), day 9 (322±47), day 12 (277±81), and day 15 (350±65). There is a significant ($p<0.001$) difference between day 0 and each of the other five time points, and between day 3 and day 15. There is also a significant difference ($p<0.01$) between day 3 and day 9.

UNIVERSITY OF CALIFORNIA LIBRARY

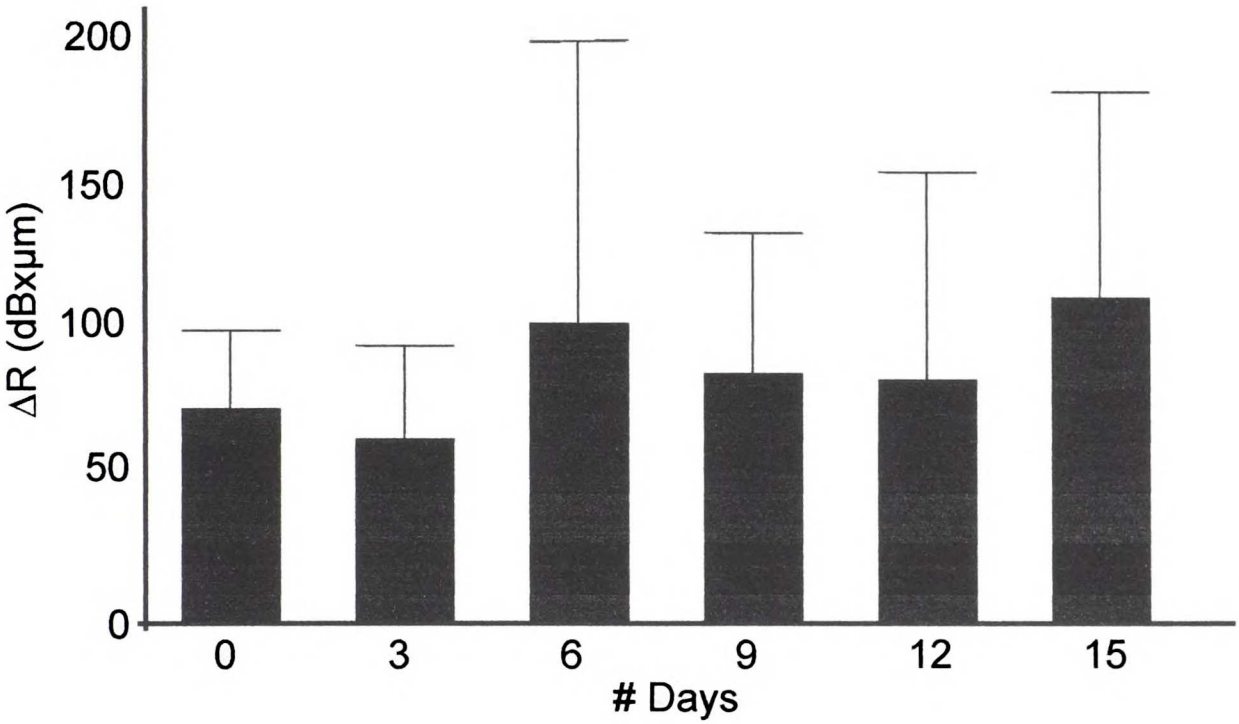

Figure 9. Mean reflectivity at days 0, 3, 6, 9, 12, and 15 for the control group when the scans were taken adjacent to the bracket base. The error bars represent standard deviations. There was no significant difference in demineralization over time.

Table 4. The average backscattering and standard deviations at days 0, 3, 6, 9, 12, and 15 for the control group.

Day	Number of Points	Mean	SD
day 0	15	58	36
day 3	15	247	66
day 6	15	306	57
day 9	15	322	47
day 12	15	277	81
day 15	15	350	65

UNIVERSITY OF CALIFORNIA LIBRARY

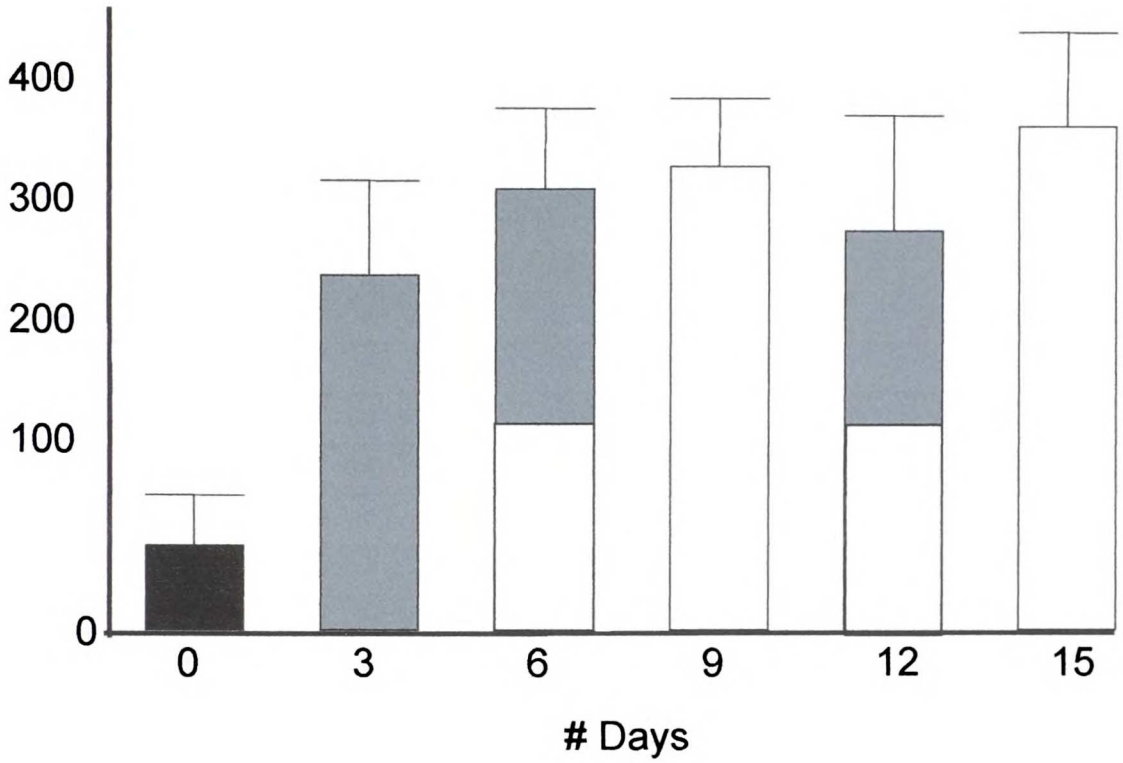

Figure 10. Mean reflectivity at days 0, 3, 6, 9, 12, and 15 for the control group. The error bars represent standard deviations. Day 0 showed significantly less demineralization than the other days. The bars with two shading patterns are not significantly different from either group containing that pattern.

Table 5 and Figure 11 display the average backscattering at days 0, 3, 6, 9, 12, and 15 for the fluoride in solution group. The greatest increase in demineralization is again seen very early on from day 0 to day 3. The demineralization then decreases with the greatest decrease at day 12. The means and standard deviations for each time point are as follows: day 0 (88±59), day 3 (236±68), day 6 (202±68), day 9 (195±69), day 12 (149±44), and day 15 (194±66). There is a significant ($p<0.001$) difference between day 0 and day 3, 6, 9 and 15, and between day 3 and day 12. There is also a significant difference ($p<0.05$) between day 0 and day 12.

Table 5. The average backscattering and standard deviations at days 0, 3, 6, 9, 12, and 15 for the fluoride in solution group.

Day	Number of Points	Mean	SD
day 0	15	88	59
day 3	15	236	68
day 6	15	202	68
day 9	15	195	69
day 12	15	149	44
day 15	15	194	66

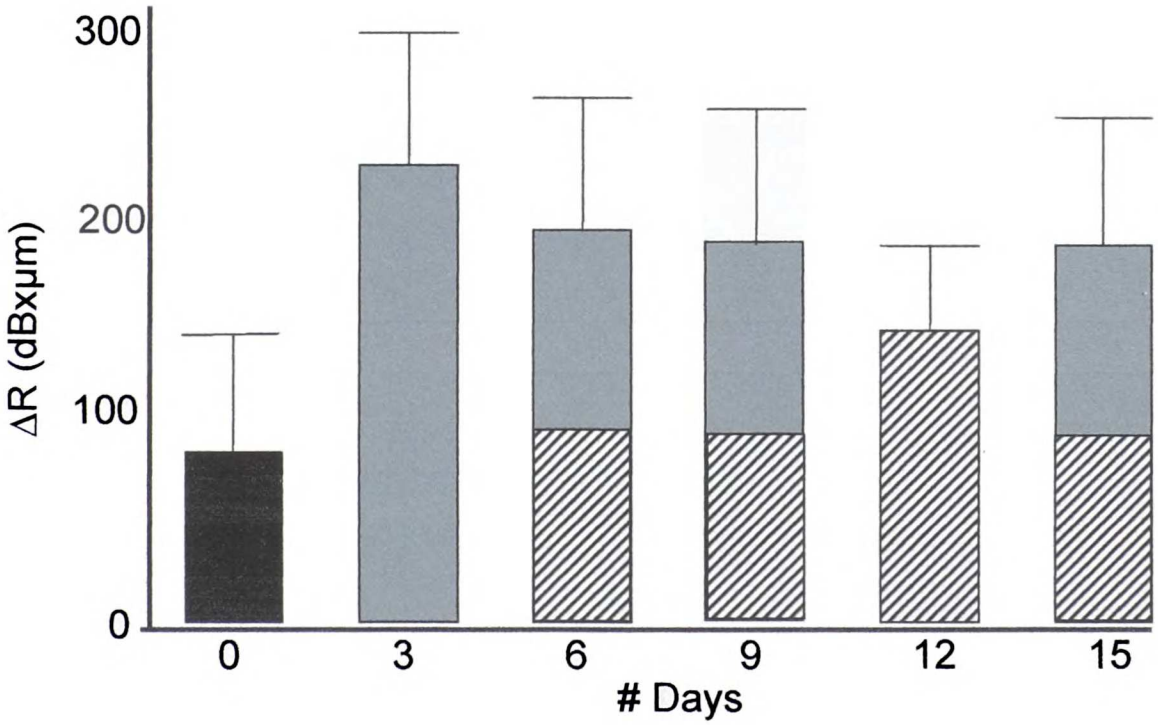

Figure 11. Mean reflectivity at days 0, 3, 6, 9, 12, and 15 for the fluoride in solution group. The error bars represent standard deviations. Day 0 is significantly different from the other groups. The bars with two shading patterns are not significantly different from either group containing that pattern.

UC SOUTHERN REGIONAL LIBRARY FACILITY

Table 6 and Figure 12 display the average backscattering at days 0, 3, 6, 9, 12, and 15 for the fluoride sealant group. The greatest increase in demineralization was not seen very early on from day 0 to day 3 as in the control and fluoride in solution groups. There was a delayed start of demineralization, then demineralization increased at day 6 and again plateaued, with a slight increase at day 12. The means and standard deviations for each time point were as follows: day 0 (53±44), day 3 (55±29), day 6 (110±39), day 9 (115±50), day 12 (136±42), and day 15 (110±33). There was a significant ($p<0.001$) difference between day 0 and day 9, between day 0 and day 12, between day 3 and day 9, and between day 3 and day 12. There is also a significant difference ($p<0.01$) between day 0 and day 6 and 15, and between day 3 and 6 and day 3 and 15.

Table 6. The average backscattering and standard deviations at days 0, 3, 6, 9, 12, and 15 for the fluoride sealant group.

Day	Number of Points	Mean	SD
day 0	15	53	44
day 3	15	55	29
day 6	15	110	39
day 9	15	115	50
day 12	15	136	42
day 15	15	110	33

UC Fran
RAF

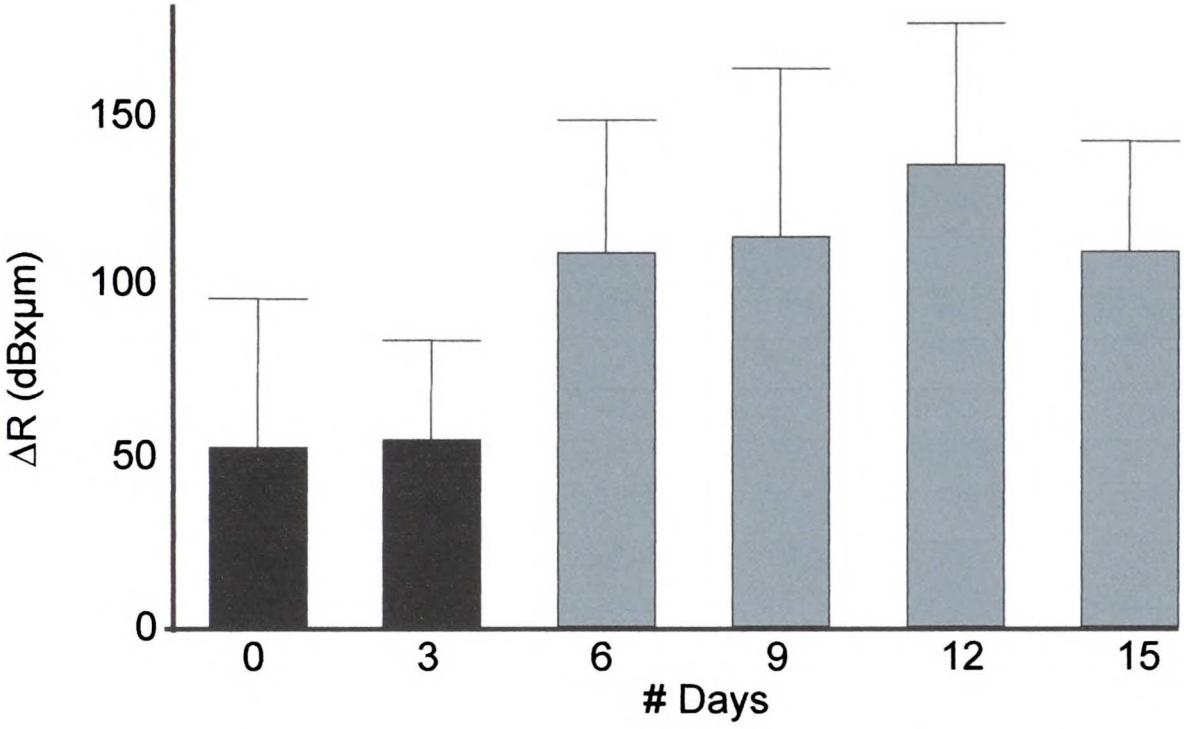

Figure 12. Mean reflectivity at days 0, 3, 6, 9, 12, and 15 for the fluoride sealant group. The error bars represent standard deviations. The same color in each bar indicates no significant difference between groups. Days 0 and 3 are significantly different from days 6, 9, 12, and 15.

Table 7 and Figure 13 display the average backscattering at days 0, 3, 6, 9, 12, and 15 for the glass ionomer group. The greatest increase in demineralization is seen very early on from day 0 to day 3 as in the control and fluoride in solution groups, but the increase is less. The means and standard deviations for each time point are as follows: day 0 (55±46), day 3 (115±47), day 6 (164±71), day 9 (176±78), day 12 (206±91), and day 15 (170±63). There is a significant ($p<0.001$) difference between day 0 and days 6, 9, 12, and 15, and between day 3 and day 12. There is also significance ($p<0.05$) between day 0 and 3, and between day 3 and 15.

UCSF LIBRARY

Table 7. The average backscattering and standard deviations at days 0, 3, 6, 9, 12, and 15 for the glass ionomer group.

Day	Number of Points	Mean	SD
day 0	15	55	46
day 3	15	115	47
day 6	15	164	71
day 9	15	176	78
day 12	15	206	91
day 15	15	169	63

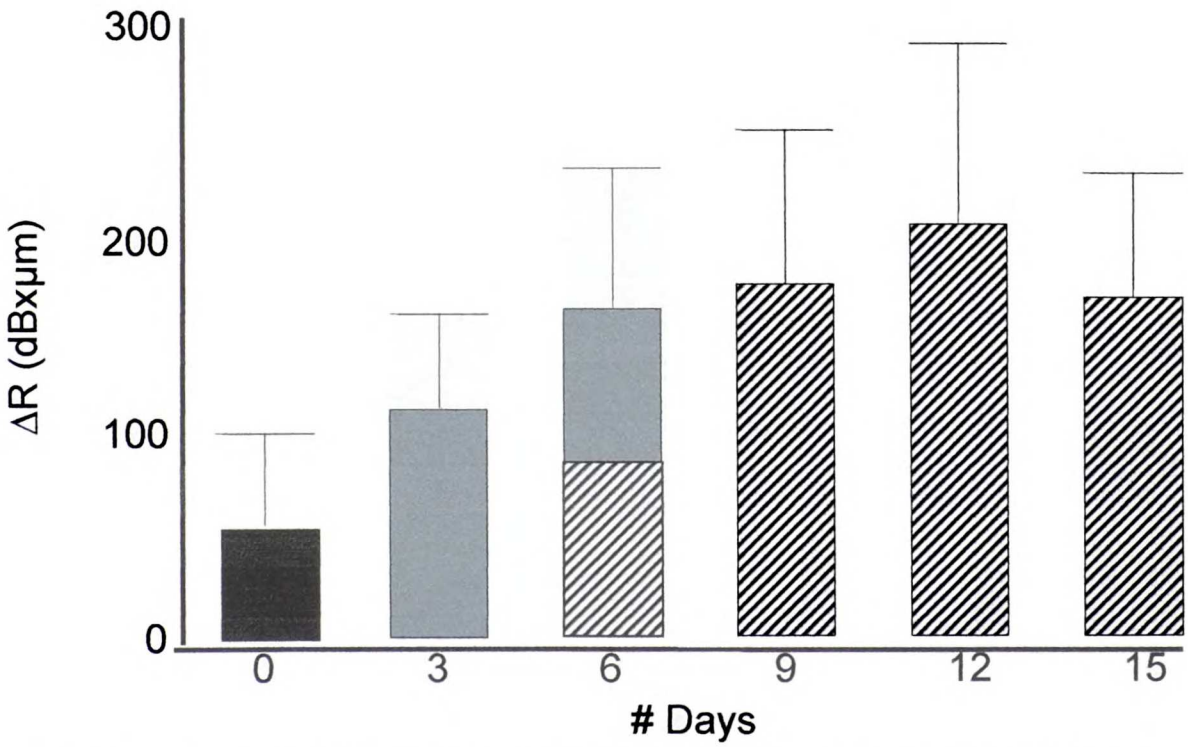

Figure 13. Mean reflectivity at days 0, 3, 6, 9, 12, and 15 for the glass ionomer group. The error bars represent standard deviations. The bars with two shading patterns are not significantly different from either group containing that pattern. Day 0 is significantly different from all other days.

UNIVERSITY OF CALIFORNIA

Figure 14 shows integrated reflectivity plotted vs. the square root of time. The backscattering observed should be proportional to the square root of time because the lesion severity is expected to increase. The integrated mineral loss is expected to increase with the square root of time since this is a diffusion-controlled process (Featherstone et al., 1983; Featherstone et al., 1986; Featherstone et al., 1990). There is an excellent linear correlation between the measured lesion severity and the square root of time (Pearson correlation coefficient = 0.93 for the control lesion without fluoride).

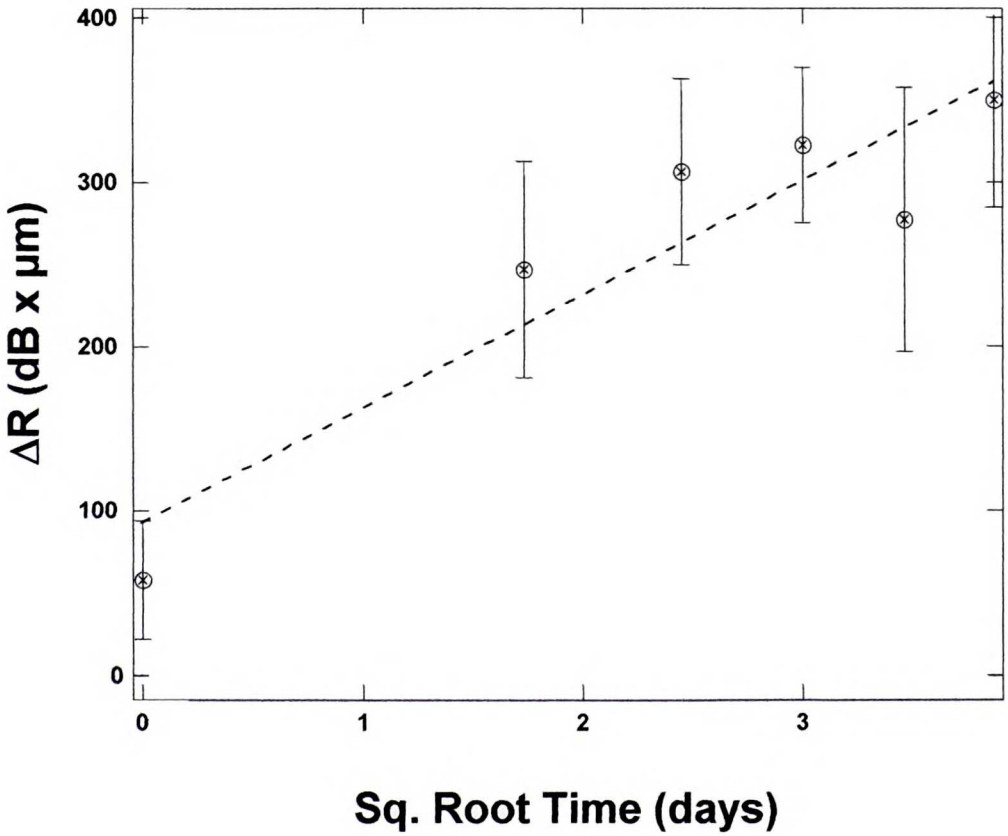

Figure 14. Integrated reflectivity plotted vs. the square root of time for the control group. The error bars represent standard deviations. An excellent linear correlation is seen.

UNIVERSITY OF CALIFORNIA LIBRARY

The microradiography data is depicted in Table 8 (appendix). The ΔZ values represent the integrated mineral loss of each sample. There were very few sections that could be analyzed by microradiography due to the loss during sectioning, and the lack of caries visually. There are 6 samples from the control group, 7 samples from the fluoride in solution group, 3 samples from the fluoride sealant group, and 2 samples from the glass ionomer group. Two sides of sample #14 were analyzed, one at 3 seconds of exposure time and one at 5 seconds.

Polarized light microscopy data is shown in Tables 9 (below) and 10 (appendix). The lesion depth for each successfully-sectioned sample was measured in micrometers. The sum and average of the measurements for each group are noted. The averages for each group were: control (177 ± 52 μm), fluoride in solution (119 ± 42 μm), fluoride sealant (87 ± 25 μm), and glass ionomer (112 ± 46 μm). The control group had the deepest lesions, followed by the fluoride in solution group, the glass ionomer group, and the shallowest lesions were seen with the fluoride sealant group. The control group exhibited significantly deeper lesions than the fluoride in solution ($p<0.01$), fluoride sealant ($p<0.001$), and glass ionomer ($p<0.05$) groups. These results are in agreement with the PS-OCT data. Due to the loss of samples mainly in the fluoride sealant and glass ionomer groups, the group averages may not be reliably compared.

UCSF LIBRARY

Table 9. Polarized light microscopy data for the four groups displaying the mean depths of the lesions and the standard deviations.

Group	Number of Points	Mean	SD
Control	15	177	52
F in Solution	15	119	42
F Sealant	15	87	25
Glass Ionomer	15	112	46

Sample comparisons for PS-OCT, microradiography, and polarized light microscopy (PLM) from each of the four groups at day 15 are displayed in Figures 15, 16, 17, and 18. Figure 15 shows an example from the control group. The dark red area on the OCT scan (a) shows that significant demineralization occurred. The PLM (b) clearly shows the lesion represented by the black area. The microradiography image (c) shows that a lesion is present. Figure 16 shows the images from the fluoride in solution group. There is still demineralization present but the intensity is less than the control group. The PLM and microradiography images again show the lesion presence. Figure 17 displays the images from the fluoride sealant group. There is a significant reduction in demineralization as compared to the control and fluoride in solution groups as seen on the OCT scan, PLM and microradiography images. Figure 18 shows images from the glass ionomer group. The extent of demineralization is greater than the fluoride sealant samples, but appears to be less than the control and fluoride in solution samples.

UCSF LIBRARY

FIGURE 15: CONTROL

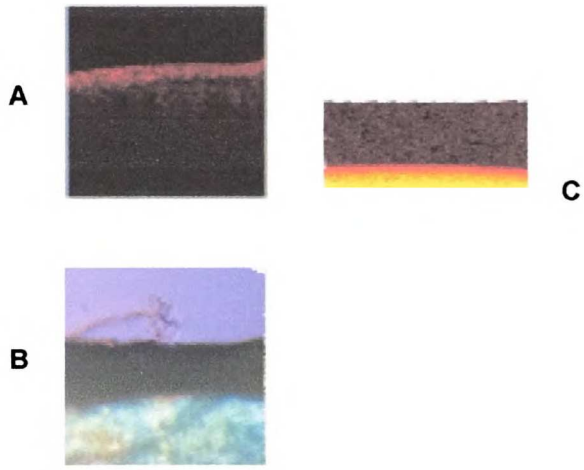

Figure 15. PS-OCT (A), PLM (B), and microradiography (C) images from a control sample. The red area on the OCT scan, the dark area on the PLM image, and the orange-red area on the microradiography image represent the carious lesion.

UCSF LIBRARY

FIGURE 16:
FLUORIDE IN SOLUTION

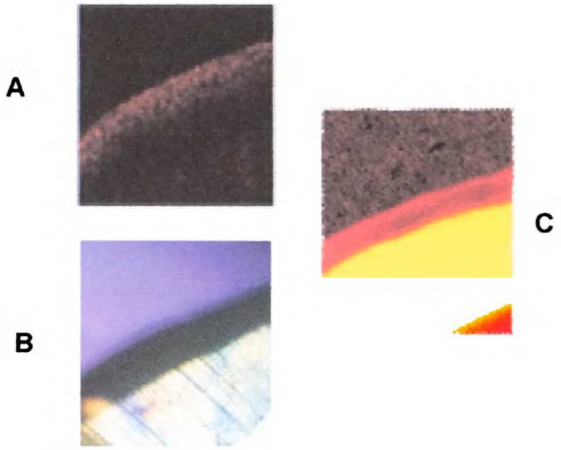

Figure 16. PS-OCT (A), PLM (B), and microradiography (C) images from a fluoride in solution sample. The red area on the OCT scan, the dark area on the PLM image, and the orange-red area on the microradiography image represent the carious lesion.

UCSF LIBRARY

FIGURE 17: FLUORIDE SEALANT

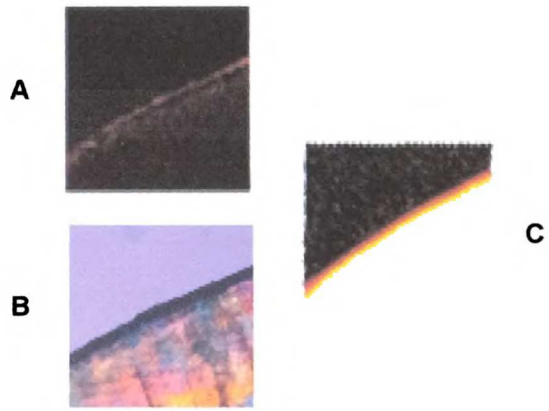

Figure 17. PS-OCT (A), PLM (B), and microradiography (C) images from a fluoride sealant sample. The red area on the OCT scan, the dark area on the PLM image, and the orange-red area on the microradiography image represent the carious lesion.

UCSF LIBRARY

FIGURE 18: GLASS IONOMER

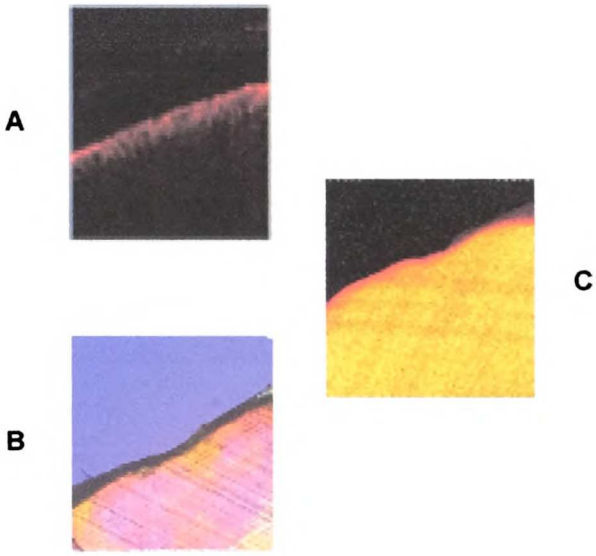

Figure 18. PS-OCT (A), PLM (B), and microradiography (C) images from a glass ionomer sample. The red area on the OCT scan, the dark area on the PLM image, and the orange-red area on the microradiography image represent the carious lesion.

UCSF LIBRARY

DISCUSSION

The specific aims of the study were to create a nondestructive imaging method to track the development of white spot lesions around orthodontic brackets, and to test the efficacy of a fluoride-releasing adhesive (glass ionomer), a fluoride sealant, and fluoride in solution in preventing decay around brackets.

This study shows that the PS-OCT system can effectively detect early demineralization on smooth surfaces around bracket bases. Initially, the OCT line profiles were taken adjacent to the left side of the bracket bases. The left side was chosen arbitrarily. Even though the cement was removed from around the base, there could have still been remnant cement that could not be seen with the naked eye. This cement could have interfered with the backscattering measured. Viewing the samples under a microscope would have helped in identifying excess cement, but clinically this would be impractical. It was then decided that the line profiles were to be taken halfway between the left side of the bracket base and the left edge of the tooth. Along a smooth surface the demineralization should be relatively uniform, so the data taken from the middle point should be the same as that taken from the side of the bracket base if all excess cement was removed. It can be argued that there may have been differences between these two points due to differences in the thickness and quality of the enamel at different areas of the tooth, but these differences would be expected to even out over all the samples in the group.

The different fluoride modalities should all provide some protection to tooth structure, so less backscattering should be seen with all fluoride groups

UCSF LIBRARY

compared to controls. It was expected that the backscattering from the control group samples would progressively increase from day 0 to day 15 as more severe demineralization occurred. For the fluoride groups, it was expected that the backscattering would decrease initially due to fluoride remineralizing tooth structure, then increase over time due to the decreased fluoride content not being able to meet the acid challenge. All fluoride groups did experience less demineralization than the control group, and the rapid increase in demineralization was halted. Demineralization was noted in all groups, signifying that fluoride does not completely protect teeth from caries but can reduce the severity of the lesions.

The PS-OCT results showed that the fluoride sealant (Proseal, Reliance Orthodontic Products) was more effective than the fluoride in solution (2ppm fluoride) and the glass ionomer cement ((Fuji Ortho LC 2-part adhesive, GC America). The control group showed a large initial increase in demineralization from day 0 to day 3, then a continual increase until day 15, which shows that the absence of fluoride allowed carious lesions to progress rapidly. This progression was consistent with a diffusion-controlled process in which the lesion severity increases as the square-root of time (Featherstone et al., 1983; Featherstone et al., 1986; Featherstone et al., 1990). Since the solutions were changed before day 9 for all samples, the only fluoride group to receive two applications of fluoride was the fluoride in solution group. The fluoride in solution group demonstrated a large initial increase in demineralization from day 0 to day 3 like the control group, followed by a progressive decrease in the demineralization as

UCSF LIBRARY

the fluoride took effect. The fluoride in solution was not the most effective fluoride modality, and probably would have been less effective with only one application.

The glass ionomer group showed the same general trend as the control group, except there was much less increase in backscattering, and a much lower maximal amount of backscattering. A possible reason for the similarity in white spot lesion development of the control and glass ionomer groups could be the way the samples were prepared. The OCT system could not image through any remnant of material so a high-speed polishing point was used to remove all cement from around the bracket. This could have removed enough glass ionomer cement for there to be leakage around the bracket base, and therefore white spot lesions developed. When the glass ionomer group was reanalyzed, the OCT results were similar to controls. This could have been because the line profiles were taken farther away from the side of the bracket and the glass ionomer cement acted only under and immediately around the bracket base. Glass ionomer has been shown to release fluoride in the immediate vicinity and be a continual source of fluoride over time (Pascotto et al., 2004, Millett et al., 1999, Ogaard et al., 1997). This could explain why the backscattering, even though similar to controls, was still less for the glass ionomer group than the control group.

The fluoride sealant group did not show the initial increase in demineralization seen with the control and glass ionomer groups. There was an immediate protective effect of the sealant, with a delayed increase in

UCSF LIBRARY

demineralization. This may be breakdown of the sealant over the 15 days. Reapplication of the fluoride sealant may have provided even greater protection from the acid attack.

The OCT results correlated with the gold standard microradiography and with the polarized light microscopy. Unfortunately, a limited sample was able to be analyzed by microradiography due to loss during sectioning. Due to the small number of samples analyzed by microradiography, a true, generalizable correlation between PS-OCT and microradiography could not be established and a ΔZ graph was not used. Figures 15, 16, 17, and 18 show that microradiography detected a lesion when the OCT system noted it existed.

Polarized light microscopy was utilized to measure the depth of the lesion as compared to PS-OCT. Figures 15, 16, 17, and 18 show that the two methods did correlate well, again supporting the hypothesis that PS-OCT is an effective method to detect white spot lesions around bracket bases.

The PS-OCT system has shown to be a good alternative to traditional radiographs and other light/optical detection methods. Before being introduced into the clinic, limitations need to be assessed. Clinically it is very difficult and often impossible to remove all of the excess cement around bracket bases when bonding. The cement, even if it is able to be imaged through, alters lesion development. The clinical probe needs to be small enough to image posterior and lingual areas. The system needs to be simple enough for easy operation. Once these issues are addressed and altered, the system will provide clinicians the ability to quickly and accurately determine whether a lesion is present,

UCSF LIBRARY

exactly where it is, and the extent of the lesion. White spot lesions are so prevalent in orthodontic patients, and early detection will prevent severe demineralization from developing and progressing.

UCSF LIBRARY

CONCLUSION

PS-OCT is an effective method to detect white spot lesions around bracket bases and quantify their severity, as verified by microradiography and polarized light microscopy. Fluoride was effective in decreasing lesion depth and extent and seemed to decrease the progression of the lesions. Fluoride sealant was the most effective fluoride modality, followed by fluoride in solution, then the glass ionomer which was the least effective modality. The clinical implication of this study is to be able to simply and accurately detect early demineralization. The area of interest could be scanned and it could be determined very quickly if demineralization exists. The clinician could also stop the initiation or progression of demineralization by applying the most effective fluoride modality, and possible reapplications of certain modalities over treatment time. It is important to monitor lesion progression or arrest, so just fluoride application without a detection method would not be advised. White spot lesions are extremely prevalent in orthodontics. It is more difficult to maintain oral hygiene with bands and brackets so caries are likely to develop around the appliances. Carbonated beverages can dissolve the cement around bands and brackets and expose tooth structure to acid attack and caries formation. Fluoride application along with early detection can minimize demineralization, enhancing esthetics and patient satisfaction.

UCSF LIBRARY

REFERENCES

Angmar-Manssona B, Al-Khateebb, Tranaeusa S (1999). Current research with quantitative light fluorescence. *Early Detection of Dental Caries II.* 4th Annual Indiana Conference May 19-22, 1999.

Anttonen V, Seppa L, Hausen H (2003). Clinical study of the use of the laser fluorescence device DIAGNOdent for detection of occlusal caries in children. *Caries Res.* 37: 17-23.

Baumgartner A, Hitzenberger CK, Dicht S, Sattmann H, Moritz A, Sperr W, Fercher AF (1998). Optical coherence tomography for dental structures. Lasers in Dentistry IV, San Jose: SPIE.

Baumgartner A, Dicht S, Hitzenberger CK, Sattmann H, Robi B, Moritz A, Sperr W, Fercher AF (1999). Polarization-sensitive optical optical coherence tomography of dental structures. Bios 99, San Jose: SPIE.

Baumgartner A, Dicht S, Hitzenberger CK, Sattmann H, Robi B, Moritz A, Sperr W, Fercher AF (2000). Polarization-sensitive optical optical coherence tomography of dental structures. *Caries Res.* 34: 59-69.

Chauncey HH, Glass RL, Alman JE (1989). Dental caries, principal cause of tooth extraction in a sample of US male adults. *Caries Res* 23: 200-205.

Colston BW, Everett MJ, Da Silva LB (1997). OCT for diagnosis of periodontal disease. San Jose: SPIE, p. 216-20.

Colston BW, Everett MJ, Da Silva LB, Otis LL, Stroeve P, Nathel H (1998a). Imaging of hard- and soft- tissue structure in the oral cavity by optical coherence tomography. *Applied Optics.* 37(16): 3582-85.

Colston BW, Sathyam US, Da Silva LB, Everett MJ (1998b). Dental OCT. *Optics Express.* 3(6): 230-238.

de Boer JF, Srinivas SM, Park BH, Pham TH, Chen Z, Milner TE, Nelson JS (1999). Polarization effects in optical coherence tomography of various biological tissues. IEEE J Sel Top in Quantum Elec 5(4): 1200-15.

Donly KJ and Segura A (2002). Fluoride release and caries inhibition associated with a resin-modified glass-ionomer cement at varying fluoride loading doses. *Am J Dent* 15(1): 8-10.

Eakle WS, Gansky SA, Zhan L, Featherstone JDB (2003). Clinical evaluation of the diagnodent device. In: Stookey GK, ed. *Early Detection of Dental Caries.* 3rd ed. Indianapolis, IN.

UCSF LIBRARY

Everett MJ, Colston BW, Sathyam US, Silva LBD, Fried D, Featherstone JDB (1999). Non-invasive diagnosis of early caries with polarization sensitive optical coherence tomography (PS-OCT). Lasers in Dentistry V, San Jose: SPIE.

Featherstone JD, Holmen L, Thylstrup A, Fredebo L, Shariati M (1985). Chemical and histological changes during development of artificial caries. *Caries Res* 19(1):1-10.

Featherstone JDB (1980). Chemistry and physiology of dental caries. *Chemistry in New Zealand.*

Featherstone JDB, ten Cate JM, Shariati M, Arends J (1983). Comparison of artificial caries -like lesions by quantitative microradiography and microhardness profiles. *Caries Res.* 17: 385-91.

Featherstone JDB, O'Reilly MM, Shariati M, Brugler S (1986). Enhancement of remineralization *in vitro* and *in vivo*. In *Factors Relating to Demineralization and Remineralization of the Teeth.* S.A. Leach, Ed., IRL, Oxford, UK.

Featherstone JDB, Glena R, Shariati M, Shields CP (1990). Dependence of *in vitro* demineralization and remineralization of dental enamel on fluoride concentration. *J Dent Res.* 69: 620-25.

Featherstone JDB (1990). An updated understanding of the mechanism of dental decay and its prevention. *Nutrition Quarterly.* 14(1): 5-11.

Featherstone JDB (1999). Prevention and reversal of dental caries: role of low level fluoride. *Community Dent Oral Epidemiol* 27: 31-40.

Featherstone JDB (2000). The science and practice of caries prevention. *JADA* 131: 887-899.

Feldchtein FI, Gelikonov GV, Gelikonov VM, Iksanov RR, Kuranov RV, Sergeev AM, Gladkova ND, Ourutina MN, Warren JA, Reitze DH (1998). In vivo OCT imaging of hard and soft tissue of the oral cavity. *Optics Express* 3(3):239-251.

Fontana M, Yanikoglu FC, Ozturk F, Ando M, Hayran O, Gonzalez-Cabezas C, Haider A, Baldridge L, Stookey GK (1996). Comparison of QLF, ultrasound, and confocal microscopy in the measurement of demineralization/remineralization of enamel lesions developed on natural smooth surfaces.

Fried D, Featherstone JDB, Glena RE, Seka W (1995). The nature of light scattering in dental enamel and dentin at visible and near-IR wavelengths. *Appl. Optics* 34(7):1278-1285.

UCSF LIBRARY

Fried D, Xie J, Shafi S, Featherstone JDB, Breunig T, Lee CQ (2002). Early detection of dental caries and lesion progression with polarization sensitive optical coherence tomography. *J. Biomed. Optics* 7(4):618-627.

Geiger AM, Gorelick L, Gwinnett AJ, Benson BJ (1992). Reducing white spot lesions in orthodontic populations with fluoride rinsing. *Am J Orthod Dentofacial Orthop* 101(5): 403-07.

Gorton J, Featherstone JD (2003). In vivo inhibition of demineralization around orthodontic brackets. *Am J Orthod Dentofacial Orthop* 123(1):10-4.

Hafstroem-Bjoerkman U, de Josselin de Jong E, Oliveby A, Angmar-Mansson B (1992). Comparison of laser fluorescence and longitudinal microradiography for quantitative assessment of *in vitro* enamel caries. *Caries. Res.* 26: 241-247.

Hale GM, Querry MR (1973). Optical constants of water in the 200-nm to 200-μm wavelength region. *Appl. Optics* 12: 555-563.

Hirce JD, Sather AH, Chao EY (1980). The effect of topical fluorides, after acid etching of enamel, on the bond strength of directly bonded orthodontic brackets. *Am J Orthod* 78(4): 444-52.

Huang D, Swanson EA, Lin CP, Schuman JS, Stinson WG, Chang W, Hee MR, Flotte T, Gregory K, Puliafito CA, Fujimoto JG (1991). Optical Coherence Tomography. *Science* 254(1178-1181.

Jones RS, Fried D (2002). Attenuation of 1310-nm and 1550-nm Laser Light through Sound Dental Enamel. Lasers in Dentistry VIII, San Jose: SPIE.

Jones RS, Staninec M, Fried D (2004). Imaging artificial caries under composite sealants and restorations. *Journal of Biomedical Optics* 9(6):1297-1304.

Kaste LM, Selwitz RH, Oldakowski RJ, Brunelle JA, Winn DM, Brown LJ (1996). Coronal caries in the primary and permanent dentition of children and adolescents 1-17 years of age: United States, 1988-1991. *J Dent Res* 75: 631-641.

Marcusson A, Norevall LI, Persson M (1997). White spot reduction when using glass ionomer cement for bonding in orthodontics: a longitudinal and comparative study. *Eur J Orthod* 19(3): 233-42.

Millett DT, Nunn JH, Welbury RR, Gordon PH (1999). Decalcification in relation to brackets bonded with glass ionomer cement or a resin adhesive. *Angle Orthod* 69(1): 65-70.

UCSF LIBRARY

Ogaard B, Rezk-Lega F, Ruben J, Arends J (1992). Cariostatic effect and fluoride release from a visible light-curing adhesive for bonding of orthodontic brackets. *Am J Orthod Dentofacial Orthop* 101(4): 303-7.

Ogaard B, Arends J, Helseth H, Dijkman G, van der Kuijl M (1997). Fluoride level in saliva after bonding orthodontic brackets with a fluoride containing adhesive. *Am J Orthod Dentofacial Orthop* 111(2): 199-02.

Otis LL, Colston BW, Everett MJ, Nathel H (2000). Dental Optical Coherence Tomography:A Comparison of Two in vitro Systems. *Dentomaxillofacial Radiology* 29(2):85-89.

Pascotto RC, de Lima Navarro MF, Filho LC, Cury JA (2004). In vivo effect of a resin-modified glass ionomer cement on enamel demineralization around orthodontic brackets. *Am J Orthod Dentofacial Orthop* 125(1): 36-41.

Rousseau C, Vaidya S, Creanor SL, Hall AF, Girkin JM, Whitters CJ, Strang R, McHugh S (2002). The effect of dentine on fluorescence measurements of enamel lesions in vitro. *Caries Res* 36(6):381-5.

ten Bosch JJ, Zijp JR (1991). Optical properties of dentin. *Dentine and Dentine Reactions in the Oral Cavity.* IRL Press Limited, Oxford, England: p. 59-65.

Thylstrup A, Bruun C, Holmen L (1994). In vivo caries models--mechanisms for caries initiation and arrestment. *Adv Dent Res* 8(2):144-57.

Wang XJ, Milner TE, de Boer JF, Zhang Y, Pashley DH, Nelson JS (1999). Characterization of dentin and enamel by use of optical coherence tomography. *Applied Optics* 38(10):2092-2096.

White JM, Eakle WS (2000). Rationale and treatment approach in minimally invasive dentistry. *JADA* 131: 13-19.

Winn DM, Brunelle JA, Selwitz RH, Kaste LM, Oldakowski RJ, Kingman A, Brown LJ (1996). Coronal and root caries in the dentition of adults in the United States, 1988-1991. *J Dent Res* 75: 642-651.

Zero DT, Mol A, Sa Roriz C, Spoon M, Jacobs A, Keem S, Elbaum M (1992). Caries detection using digital imaging fiber-optic transillumination (DIFOTI): A preliminary evaluation. In: Stookey GK, ed. *Early Detection of Dental Caries II.* Indianapolis, IN.

UCSF LIBRARY

APPENDIX

Table 1. PS-OCT reflectivity data for the control, fluoride in solution, fluoride sealant, and glass ionomer groups. The data is arranged by sample number and days of experimentation. The values are expressed in decibels x μm (ΔR).

POLARIZATION-SENSITIVE OPTICAL COHERENCE TOMOGRAPHY

GROUP	SAMPLE	DAYS 0	3	6	9	12	15
CONTROL	1	53.5	143.2	236.8	290.4	289.9	322.7
	2	101.8	269.3	351.6	347.2	277.4	346.2
	3	43.1	294.8	383.1	323.5	350.5	342.4
	4	93.6	299.0	363.5	309.8	52.9	418.0
	5	9.3	224.9	271.1	274.5	222.8	280.3
	6	108.9	323.2	310.5	398.6	328.1	389.9
	7	35.4	252.8	345.0	309.8	372.5	170.6
	8	19.5	230.7	344.1	359.8	316.7	424.5
	9	14.4	156.1	314.0	325.8	247.4	347.4
	10	31.5	297.9	190.0	368.4	314.0	424.7
	11	49.7	220.5	257.9	286.2	213.3	343.6
	12	69.6	327.7	359.2	374.2	311.6	324.2
	13	100.1	254.4	334.2	363.6	352.4	386.5
	14	108.3	115.1	297.3	219.2	204.2	329.5
	15	35.8	292.9	235.9	283.2	298.8	397.9
FLUORIDE IN SOLN	16	35.3	132.9	177.0	214.0	250.9	183.1
	17	50.5	165.8	187.1	199.0	196.5	201.3
	18	75.8	135.0	151.3	166.7	180.6	130.6
	19	23.1	242.6	242.1	109.3	136.6	189.3
	20	131.9	245.0	292.8	83.3	166.7	162.0
	21	200.9	339.1	311.4	335.4	137.3	223.7
	22	109.1	189.1	209.2	199.6	124.8	90.0
	23	69.7	182.5	118.5	107.4	92.3	118.5
	24	160.0	277.5	271.3	287.3	92.4	349.0
	25	71.4	346.4	267.5	247.1	186.5	182.9
	26	87.8	209.3	71.1	184.3	108.6	215.2
	27	15.4	270.6	215.9	182.1	168.8	286.0
	28	34.2	250.9	155.3	223.9	164.8	176.7
	29	191.0	321.4	220.0	250.6	103.1	249.3
	30	59.5	227.4	140.9	138.1	130.4	145.2
FLUORIDE SEALANT	31	148.8	53.2	162.3	167.0	195.1	97.1
	32	118.4	68.6	82.4	40.8	89.6	86.8
	33	96.8	30.5	62.8	166.0	133.0	78.5
	34	110.1	40.6	114.6	118.4	148.7	93.5
	35	20.7	11.8	19.6	196.9	182.4	120.8
	36	41.6	5.9	162.5	153.9	187.6	173.8
	37	35.1	79.5	95.2	179.5	120.5	110.4
	38	56.1	80.1	95.1	99.4	74.1	100.3

UCSF LIBRARY

	39	10.0	6.1	109.4	67.9	101.5	73.8
	40	30.0	88.3	137.6	116.1	125.9	121.7
	41	15.2	69.5	92.9	84.1	130.6	136.7
	42	32.3	55.3	97.4	88.1	120.9	72.0
	43	21.1	67.1	124.7	129.8	92.7	117.2
	44	33.0	77.3	135.7	57.6	213.5	178.3
	45	20.3	90.0	157.9	54.6	122.5	93.4
GLASS	46	61.2	94.0	143.3	197.5	195.8	183.4
IONOMER	47	57.2	71.3	173.0	197.0	281.5	215.0
	48	64.5	155.4	219.6	119.1	51.1	161.4
	49	14.3	66.1	56.2	72.0	102.7	100.2
	50	66.3	98.5	172.3	159.7	199.3	192.1
	51	23.0	91.3	92.1	89.3	213.5	84.9
	53	17.9	195.7	265.8	154.9	225.0	115.5
	55	29.9	156.7	207.6	205.7	233.7	256.0
	56	17.6	125.3	184.1	30.0	232.2	144.1
	57	25.3	44.1	65.2	126.9	20.6	146.6
	58	173.1	155.2	161.6	237.3	302.3	232.7
	59	88.7	167.8	285.5	311.6	289.0	255.0
	60	45.1	145.3	223.8	248.9	233.6	218.8
	61	129.7	100.9	132.0	253.8	346.3	187.2
	62	16.3	50.1	78.0	235.5	159.9	49.3

UCSF LIBRARY

Table 8. The ΔZ values (vol% mineral loss x μm) for the microradiography data represent the integrated mineral loss of each sample. There are six samples from the control group, seven samples from the fluoride in solution group, three samples from the fluoride sealant group, and two samples from the glass ionomer group.

MICRORADIOGRAPHY

	Sample	Exposure time	ΔZ (vol% x μm)
CONTROL	52	7sec	61
	6	7sec	729
	8	6sec	2111
	11	6sec	1478
	14	3sec	2075
	14	5sec	2716
F IN SOLUTION	16	5sec	2138
	18	5sec	2440
	21	5sec	1025
	22	5sec	2947
	23	6sec	2421
	24	7sec	2296
	27	7sec	2982
F SEALANT	35	4sec	1906
	37	7sec	2292
	42	5sec	933
GLASS IONOMER	48	6sec	1080
	60	5sec	2096

UCSF LIBRARY

Table 10. The polarized light microscopy data is shown. The lesion depth for each successfully-sectioned sample was measured in micrometers. The average of the measurements for each group are noted.

Polarization Light Microscopy

Group	Sample	Lesion Depth (μm)
CONTROL	1	139.1
(n=15)	2	256.9
	3	248.8
	4	117.7
	5	167.7
	6	204.8
	7	211.5
	8	146.4
	9	196
	10	210.3
	11	205.8
	12	175.4
	13	173.8
	14	56.6
	15	138.1
	Total	2648.9
	Average	176.6
FLUORIDE	16	86.8
IN SOLN	17	144
(n=13)	18	112
	19	181.6
	20	197.6
	21	101.25
	22	157.5
	23	117.9
	24	73.6
	25	123.8
	27	100
	28	45
	30	110.3
	Total	1551.35
	Average	119.3
FLUORIDE	35	60.4
SEALANT	37	86.8

UCSF LIBRARY

(n=8)	39	118
	40	59.7
	42	88.3
	43	59.1
	44	117.4
	45	107.5
	Total	697.2
	Average	87.1
GLASS IONOMER	48	181.5
(n=8)	50	135.6
	51	94.5
	53	74.7
	55	175.2
	56	66.2
	58	73
	60	98.4
	Total	899.1
	Average	112.4

UCSF LIBRARY

1644R

UCSF LIBRARY

7487773
3 1378 00748 7773
For reference
Not to be taken from the room.